DONG THAP UNIVERSITY JOURNAL OF SCIENCE
Tạp chí Khoa học Đại học Đồng Tháp
Natural Sciences Issue
ISSN 0866-7675 | e-ISSN 2815-567X

DOI: https://doi.org/10.52714/dthu.14.5.2025.1495

PREPARING AND EVALUATING RHODAMINE B REMOVAL ABILITY IN AQUEOUS SOLUTIONS OF COPPER OXIDE NANOPARTICLES

Pham Dinh Du

Thu Dau Mot University, 6 Tran Van On St., Thu Dau Mot city, Binh Duong, 75000, Vietnam
Corresponding author, Email: dupd@tdmu.edu.vn
Article history
Received: 11/02/2025; Received in revised form: 23/02/2025; Accepted: 26/02/2025

Abstract

In this paper, nanostructured copper oxide materials were prepared in N'N-dimethylformamide solvent from $Cu(NO_3)_2{\cdot}3H_2O$ and benzene-1,4-dicarboxylic acid precursors. The obtained copper oxide nanoparticles were characterized by X-ray diffraction (XRD), Fourier transform infrared spectroscopy (FT-IR), thermogravimetric analysis (TG/dTG), nitrogen adsorption-desorption isotherms, scanning and transmission electron microscopy (SEM and TEM). At 120°C synthesis, the CuO crystalline phase was mainly formed, while at 180–220°C, the Cu_2O and Cu crystalline phases were also formed in addition to the CuO crystalline phase. The adsorption or degradation ability based on H_2O_2/catalyst system of copper oxide nanoparticles for rhodamine B removal was also evaluated. The results showed that copper oxide nanoparticles had low adsorption capacity for rhodamine B, but high catalytic activity to decompose rhodamine B in aqueous solution with hydrogen peroxide as the oxidizing agent.

Keywords: *Benzene-1.4-dicarboxylic acid, copper oxide, nanoparticle, rhodamine B.*

Cite: Pham, D. D. (2025). Preparing and evaluating of rhodamine B removal ability in aqueous solutions of copper oxide nanoparticles. *Dong Thap University Journal of Scieence, 14*(5), 51-59. https://doi.org/10.52714/dthu.14.5.2025.1495

ĐIỀU CHẾ VÀ ĐÁNH GIÁ KHẢ NĂNG LOẠI BỎ RHODAMINE B TRONG DUNG DỊCH NƯỚC CỦA HẠT NANO COPPER OXIDE

Phạm Đình Dũ

Trường Đại học Thủ Dầu Một, 6 Trần Văn Ơn, Thủ Dầu Một, Bình Dương, 75000, Việt Nam
Tác giả liên hệ, Email: dupd@tdmu.edu.vn
Lịch sử bài báo
Ngày nhận: 11/02/2025; Ngày nhận chỉnh sửa: 23/02/2025; Ngày duyệt đăng: 26/02/2025

Tóm tắt

Trong bài báo này, vật liệu có cấu trúc nano copper oxide đã được điều chế trong dung môi N'N-dimethylformamide từ tiền chất $Cu(NO_3)_2{\cdot}3H_2O$ và benzene-1,4-dicarboxylic acid. Nano copper oxide thu được đã được đặc trưng bằng nhiễu xạ tia X (XRD), phổ hồng ngoại biến đổi Fourier (FT-IR), phân tích nhiệt trọng lượng (TG/dTG), đẳng nhiệt hấp phụ-khử hấp phụ nitrogen, hiển vi điện tử quét và truyền qua (SEM và TEM). Ở nhiệt độ tổng hợp 120°C, pha tinh thể CuO được hình thành là chủ yếu. Ở nhiệt độ tổng hợp 180–220°C, pha tinh thể Cu_2O và Cu cũng được hình thành bên cạnh pha tinh thể CuO. Khả năng hấp phụ hay phân hủy dựa trên hệ H_2O_2/xúc tác của nano copper oxide để loại bỏ rhodamine B cũng đã được đánh giá. Kết quả cho thấy hạt nano copper oxide có dung lượng hấp phụ thấp đối với rhodamine B, nhưng có hoạt tính xúc tác cao để phân hủy rhodamine B trong dung dịch nước với hydogen peroxide là tác nhân oxi hóa.

Từ khóa: *Benzene-1,4-dicarboxylic acid, copper oxide, hạt nano, rhodamine B.*

1. Introduction

Copper oxide nanoparticles are one of the simple oxides possessing unique physical, chemical, optical and thermal properties. Copper oxide nanoparticles are used in various applications such as catalysts, gas sensors, energy, preparation of organic/inorganic nanocomposites, electronics, machinery, construction, biological and medical fields (Bonthula et al., 2023; Fakhree et al., 2021; Rotti et al., 2022). Various methods have been proposed to produce copper oxide nanoparticles with different sizes and shapes such as thermal oxidation, sonochemical, combustion, sol-gel method, co-precipitation and hydrothermal method (Jadhav, 2021; Rotti et al., 2022). Nanomaterial properties are subject to the nanopowder size, morphology and specific surface area of the prepared material. Some aspects are strongly dependent on the preparing methods (Jadhav, 2021). In recent years, green synthesis methods using organic precursors have been of interest to many scientists and have been used in the synthesis of metal oxide nanoparticles, such as plant extracts (Rotti et al., 2022), quercetin (Fakhree et al., 2021), ascorbic acid (Espinosa-Lagunes et al., 2022). In the present work, the main objective was to synthesize copper oxide nanoparticles based on Cu(II)–benzenedicarboxylate, using benzene-1,4-dicarboxylic acid as reducing and capping agent. Copper oxide nanoparticles were characterized by various methods such as XRD, FT-IR, TG/dTG, SEM, TEM and BET.

In recent decades, water pollution by dyes and pigments has been a concern for the development of communities. The removal of dyes and pigments from wastewater has become a major research direction in the field of water pollution treatment. This is because water contaminated with dyes and pigments, even at very low concentrations, can cause many adverse effects on the aquatic environment (Park et al., 2007). Moreover, the molecules of many dyes are very stable, not degraded by light, chemicals, biology and other agents, and can affect human health (Crini, 2006). Rhodamine B (RhB) is a basic, red dye in the Xanthene class and is readily soluble in water. Xanthene dyes are among the oldest and most widely used synthetic dyes. Xanthene dyes tend to be fluorescent, producing bright colors ranging from pinkish yellow to blue-red. RhB is widely used as a dye in textiles, foods, medicines (for animals), and in the staining of biological samples. It is also a fluorescent marker for water. Improper disposal of this dye prevents sunlight from penetrating water, leading to serious environmental problems and is toxic and carcinogenic to living organisms. Therefore, its removal from wastewater is essential (Barros et al., 2023). The removal efficiency of RhB from aqueous solution via adsorption or degradation based on the H_2O_2/catalyst system of the copper oxide nanoparticle will be evaluated in this study.

2. Experimental

2.1. Chemicals and material characterization methods

Copper(II) nitrate trihydrate ($Cu(NO_3)_2{\cdot}3H_2O$, Merck, India), benzene-1,4-dicarboxylic acid ($C_8H_6O_4$, Acros, Belgium), N'N-dimethylformamide (C_3H_7NO, Fisher, Korea), hydrogen peroxide 30% (H_2O_2, Fisher, Korea) and rhodamine B ($C_{28}H_{31}O_3N_2Cl$, HiMedia, India) are pure chemicals and are used without further purification.

The XRD analysis was performed on a VNU-D8 Advance Bruker (Germany) anode X-ray diffractometer with CuKα (λ = 1.5406 Å) radiation. SEM images were obtained on an SEM JMS-5300LV (Japan). TEM images were photographed by using a JEM-2100, and FT-IR analyses were performed on a Jasco FT/IR–4600 spectrometer (Japan). Thermogravimetric analysis (TG/dTG) was performed on a Labsys TG/dTG SETARAM. Nitrogen adsorption-desorption isotherms were obtained by using a Tristar 3000 analyzer.

The samples were degassed at 170 °C with N_2 for 7 hours. The specific surface area of the samples was calculated with the Brunauer-Emmett-Teller (BET) method.

2.2. Preparing copper oxide nanoparticles

Preparing copper oxide nanoparticle was referred to and adapted from that reported by Nikravesh et al. (2023): A mixture of $Cu(NO_3)_2{\cdot}3H_2O$ (1.45 g, 6 mmol), benzene-1,4-dicarboxylic acid (1 g, 6 mmol), and N'N-dimethylformamide (DMF, 75 mL) was stirred for 20 min to form a homogeneous solution. Then, the mixture was transferred into a 100 mL Teflon-lined steel autoclave and placed in an oven at 120–220ºC for 6–72 hours. The blue precipitate was collected, washed with DMF several times, dried, and calcined at 280°C for 8 hours to obtain copper oxide nanomaterial.

The effect of ultrasonic conditions was also investigated by ultrasonicating the mixture for 20 minutes before placing it in the Teflon vessel using a SONICS Vibra-cell ultrasonicator. The subsequent steps were also performed according to the above procedure.

The synthesis conditions and sample symbols are presented in Table 1.

Table 1. Synthesis conditions and sample symbols

Sample	Synthesis temperature (ºC)	Synthesis time (hours)	Note
M-1	120	6	–
M-2	120	24	–
M-3	120	72	–
M-4	120	6	Ultrasound in 20 min.
M-5	180	6	–
M-6	180	24	–
M-7	220	6	–

2.3. Evaluating RhB removal ability in aqueous solution

The adsorption capacity of copper oxide nanoparticle was evaluated by taking 0.05 g of the material and putting it into an Erlenmeyer flask containing 50 mL of RhB solution with a concentration of 10 mg/L, shaking it with a shaker at ambient temperature for 2 hours to achieve adsorption-desorption equilibrium. Then, filter, take the solution to determine the remaining RhB concentration by UV-Vis method on Jasco V-770 (Japan) at λ_{max} = 554 nm.

The catalytic activity of copper oxide nanoparticle was also evaluated using the same procedure as above, but in the presence of hydrogen peroxide at a concentration of 6.6 g/L.

The RhB removal efficiency, *H*%, was calculated according to equation (1).

$$H\% = \frac{(A_0 - A_c)}{A_0} \times 100. \quad (1)$$

where A_0 and A_c are the absorbance at λ_{max} of RhB in the initial solution and at the end of the experiment.

3. Results and discussion

3.1. Effect of synthesis time and sonication

Figure 1 shows the X-ray diffraction patterns of M-1, M-2 and M-3 samples processed at different synthesis times (6–72 h at 120°C). It can be seen that the diffraction peaks in all

three samples are similar with high intensity and sharpness. These are the characteristic diffraction peaks of CuO (JCPDS No. 00-048-1548). Similar results were obtained for M-4 sample (Figure 1). However, M-4 sample had slightly higher diffraction peak intensities than M-1 sample (these two samples were the same synthesis time of 6 h). This suggests that sonication did not significantly affect the phase composition of the material. In this case, no peaks characteristic of the Cu(II)–benzenedicarboxylate metal-organic framework structure were observed as reported by Nikravesh et al. (2023), but only copper(II) oxide was formed with high crystallinity. Thus, it can be assumed that benzene-1,4-dicarboxylic acid acted as a reducing and capping agent to protect the formation of copper oxide nanoparticles under these conditions.

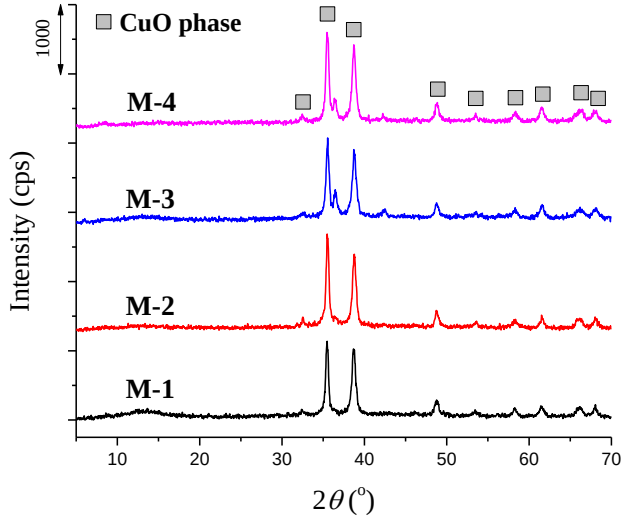

Figure 1. XRD patterns: M-1, M-2, M-3 and M-4 samples

3.2. Effect of synthesis temperature and synthesis time

The XRD patterns of the samples prepared at 180°C and different synthesis times (6 and 24 hours) are shown in Figure 2a. Observation of the patterns shows that the crystalline phase of copper(I) oxide (Cu_2O, JCPDS No. 00-005-0667) is also formed besides the crystalline phase of copper(II) oxide (CuO). The extension of the synthesis time only makes the intensity of the diffraction peaks of M-6 sample significantly higher than that of M-5 sample, indicating the high crystallinity of the phases present in the material.

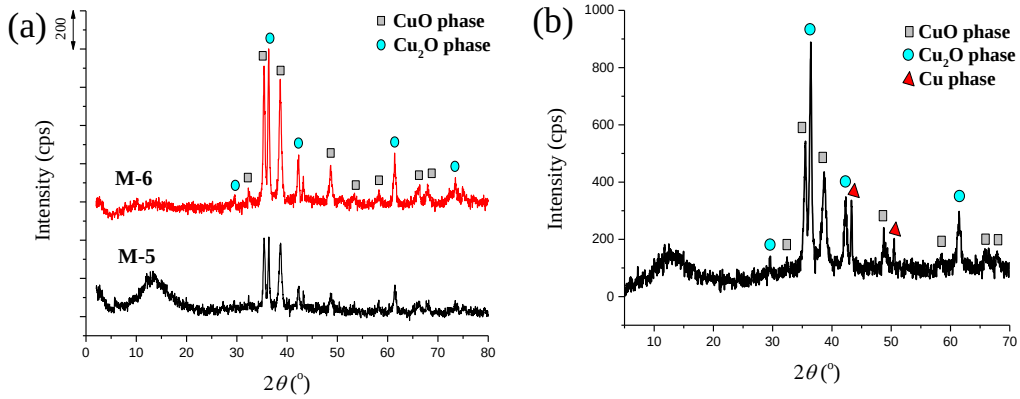

Figure 2. XRD patterns: a) M-5 and M-6 samples; b) M-7 sample

At the synthesis temperature of 220°C (Figure 2b), in addition to the crystalline phases of copper(I) oxide and copper(II) oxide, diffraction peaks characteristic of metallic Cu crystals (JCPDS No. 01-070-3039) also appeared. This showed that there were different crystalline phases of copper in the M-7 sample. The reason could be attributed to the strong reduction of Cu(II) ions at high synthesis temperatures.

The thermogravimetric analysis profiles of M-7 sample show that a small mass loss (0.94%) occurred at a temperature of about 746°C (Figure 3a). This mass loss may be due to the combustion of organic fragments embedded in the material. This indicates that a small amount of benzene-1,4-dicarboxylic acid molecules bonded to the copper ions and acted as a coating to protect the formation of copper metal crystals.

Figure 3b shows the FT-IR spectra of M-2, M-6 and M-7 samples. It can be seen that these samples have similar absorption bands. The absorption bands at 3437 and 1630 cm^{-1} are attributed to the stretching and bending vibrations of the O–H bonds of freely adsorbed water molecules. The vibrational bands in the region of 533–419 cm^{-1} are attributed to the bending vibration of the Cu–O bond (Fakhree et al., 2021; Nikravesh et al., 2023). The sharp absorption band at 1383 cm^{-1} belongs to the stretching vibration of the carboxylate group (Nikravesh et al., 2023). This also suggests that a small amount of organic molecules are attached to the copper oxide nanoparticles.

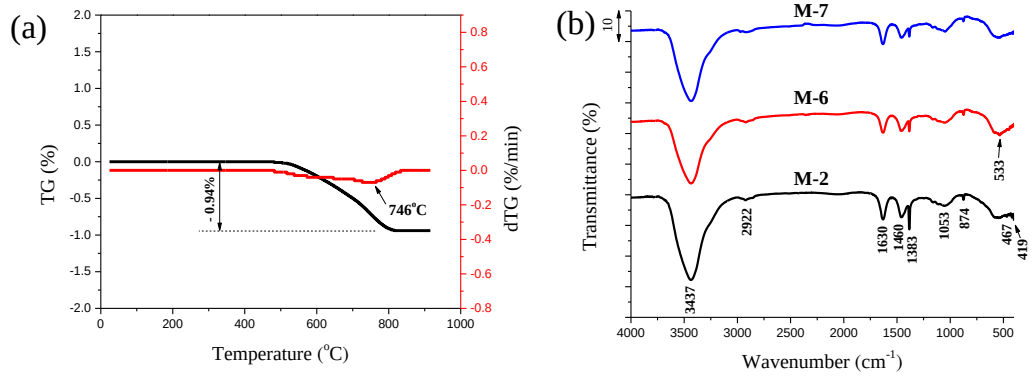

Figure 3. a) TG/dTG profiles of M-7 sample;
b) FT-IR spectra of M-2, M-6, and M-7 samples

3.3. RhB removal efficiency in aqueous solution

Figure 4a shows that M-1, M-2, M-3 and M-4 samples hardly adsorbed RhB. The removal efficiency was about 3–6% under the condition of only the material in 10 mg/L RhB solution. However, the RhB removal efficiency was quite high (48–57%) in the presence of H_2O_2. This indicates that M-1, M-2, M-3 and M-4 samples all had catalytic activity for the RhB decomposition reaction with H_2O_2 as the oxidizing agent. In which, the efficiency achieved by M-2, M-3 and M-4 samples was almost the same (56–57%), while that of M-1 sample was slightly lower (48%). The reason may be that M-2, M-3 and M-4 samples have high crystallinity and therefore high catalytic activity, while M-1 sample has a slightly lower crystallinity than the above samples (Figure 1).

The catalytic activity of M-5, M-6 and M-7 samples was also evaluated through the degradation efficiency of RhB in aqueous solution with H_2O_2 used as an oxidizing agent. The results presented in Figure 4b show that these samples all have high catalytic activity. In particular, the RhB degradation efficiency on M-6 sample reached the highest value (64%). This can be explained by the fact that M-6 sample simultaneously contains two phases of

CuO and Cu_2O with high crystallinity (Figure 2a), which may be the reason for the increased catalytic activity of the material. Therefore, M-6 sample continued to be used to analyze some characteristic properties of the material.

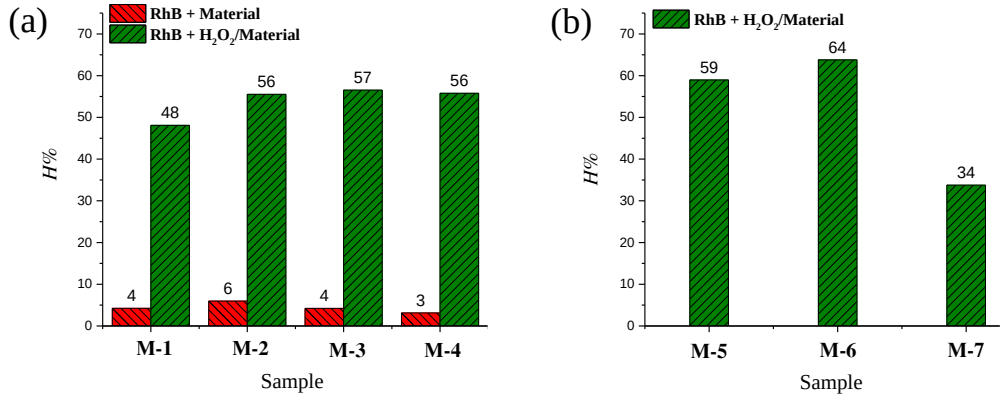

Figure 4. RhB removal efficiency of the material samples under different experimental conditions: a) M-1, M-2, M-3, and M-4 samples; b) M-5, M-6, and M-7 samples

3.4. Some characteristic properties of the material

The nitrogen adsorption-desorption analysis and morphology results of M-6 sample are presented in Figure 5.

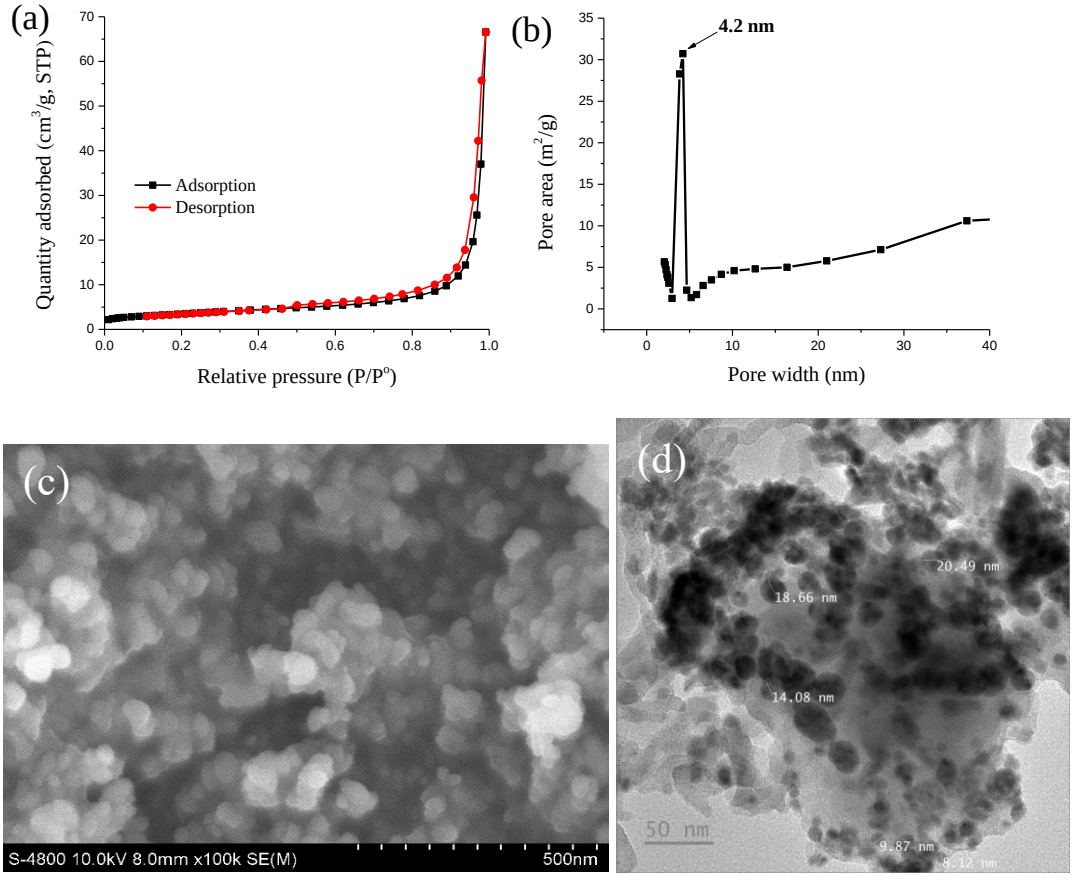

Figure 5. Nitrogen adsorption-desorption isotherms (a), pore size distribution curve (b), SEM (c), and TEM (d) images of M-6 sample

Figure 5a shows that the nitrogen adsorption isotherm of M-6 sample belongs to type III according to the IUPAC classification, which is typical for non-porous materials. Indeed, the XRD analysis results of M-6 sample show that the phase composition of the material is mainly copper oxides, including CuO and Cu_2O. Figure 5a also shows that M-6 sample has a condensation at high relative pressure ($P/P^o \sim 1$), which is the condensation in the pores formed between the material particles. The pore size distribution curve presented in Figure 5b shows that M-6 sample contains pores with a size of about 4.2 nm. The specific surface area determined by the BET method of M-6 sample is 12.3 m^2/g. This specific surface area is relatively large compared to nano-sized materials. The BET surface areas of Cu_2O and CuO nanoparticles were found to be 3.3 and 1.3 m^2/g, respectively, by Topnani et al. (2009).

SEM and TEM images of M-6 sample showed that the material consisted of well-dispersed, non-aggregated spherical particles with an average diameter of 14.2 ± 2.4 nm with a range of 8.12–20.49 nm (Figure 5 c and d). Table 2 describes the copper oxide nanoparticle products synthesized from different precursors and solvents. It can be seen that the copper oxide nanoparticle formed in this study has a relatively smaller particle size compared to many other publications.

Table 2. Description of copper oxide nanoparticle products synthesized under different conditions

Synthesized nanomaterial	Solvent	Precursor	Reducing agent	Product description	Ref.
CuO	Water	$CuSO_4$	The leaf extracts of Mangifera indica, Azadirachta indica and Carica papaya	Irregular shaped particles layered structure	(Rotti et al., 2022)
CuO	Water	$CuSO_4 \cdot 5H_2O$	Quercetin, NaOH	14.78 nm	(Fakhree et al., 2021)
CuO	Water	$CuCl_2 \cdot 2H_2O$	Acetic acid, NaOH	16.57 nm	(Jadhav, 2021)
CuO	Benzene and hexane	$CuCl_2 \cdot H_2O$	KOH	32 nm	(Topnani et al., 2009)
Cu_2O	Water	CuCl	KOH	31 nm	(Topnani et al., 2009)
Cu/Cu_2O	Ethylene glycol	$CuSO_4$	Ascorbic acid, poly vinylpyrrolidone	4–10 nm	(Espinosa-Lagunes et al., 2022)
CuO/Cu_2O	DMF	$Cu(NO_3)_2 \cdot 3H_2O$	Benzene-1,4-dicarboxylic acid	14.2 nm	In this study

4. Conclusions

Copper oxide nanoparticles were successfully synthesized by the solvothermal method from $Cu(NO_3)_2 \cdot 3H_2O$ and benzene-1,4-dicarboxylic acid precursors in DMF solvent. CuO crystals were mainly formed at a synthesis temperature of 120°C. At 180–220°C synthesis, Cu_2O and Cu crystals were also formed besides the CuO crystalline phase. The obtained copper oxide nanoparticles had an average diameter of 14.2 nm and a specific surface area of 12.3 m^2/g. The copper oxide nanoparticles also had catalytic ability in the H_2O_2/catalyst reaction system to decompose RhB in aqueous solution. The decomposition

efficiency reached 64% (experimental conditions: 50 mL of RhB solution with concentration of 10 mg/L, H_2O_2 with concentration of 6.6 g/L, 0.05 g of the material, ambient temperature).

References

Barros, T. R. B., Barbosa, T. S. B., Barbosa, T. L. A., & Rodrigues, M. G. F. (2023). Adsorption of Rhodamine-B (RhB) and Regeneration of MCM-41 Mesoporous Silica. *Catalysis Research*, *3*(1). https://doi.org/10.21926/cr.2301010

Bonthula, S., Bonthula, S. R., Pothu, R., Srivastava, R. K., Boddula, R., Radwan, A. B., & Al-Qahtani, N. (2023). Recent Advances in Copper-Based Materials for Sustainable Environmental Applications. *Sustain. Chem.*, *4*, 246–271. https://doi.org/10.3390/suschem4030019

Crini, G. (2006). Non-convention allow-cost adsorbents for dye removal: a review. *Bioresour. Technol.*, *97*, 1061–1085. https://doi.org/10.1016/j.biortech.2005.05.001

Espinosa-Lagunes, F. I., Cruz, J. C., Vega-Azamar, R. E., Murillo Borbonio, I., Torres González, J., Escalona Villalpando, R. A., Gurrola, M. P., Ledesma García, J., & Arriaga, L. G. (2022). Copper nanoparticles suitable for bifunctional cholesterol oxidation reaction: harvesting energy and sensor. *Mater. Renew. Sustain Energy*, *11*, 105–114. https://doi.org/10.1007/s40243-022-00210-7

Fakhree, F. M., Waheed, I. F., & Mahmoud, K. M. (2021). Synthesis and Characterization of CuO Nanoparticles Stabilized by Quercetin and Its Application for Anti-Breast Cancer Activity. *Egyptian Journal of Chemistry*, *64*(6), 2989–2995. https://doi.org/10.21608/ejchem.2021.56260.3207

Jadhav, M. (2021). CuO Nanoparticles Synthesis by Sol- gel Method and Characterization. *Nano Sci. & Nano Technol.*, *15*(2), 106.

Nikravesh, N. Y., Beygzadeh, M., & Adl, M. (2023). Microporous MOF-5@AC and Cu-BDC@AC Composite Materials for Methane Storage in ANG Technology. *Hindawi-International Journal of Energy Research*. https://doi.org/10.1155/2023/2282746

Park, C., Lee, M., Lee, B., Kim, S. W., Chase, H. A., Lee, J., & Kim, S. (2007). Biodegradation and biosorption for decolorization of synthetic dyes by Funalia trogii. *Biochem. Eng. J.*, *36*, 59–65. https://doi.org/10.1016/j.bej.2006.06.007

Rotti, R. B., Ramya, M., Babu, K. R. V., & Sunitha, D. V. (2022). Effect of plant extracts on structural & morphological features of CuO nano structured material. *IOP Conf. Ser.: Mater. Sci. Eng.*, *1221*(012055). https://doi.org/10.1088/1757-899X/1221/1/012055

Topnani, N., Kushwaha, S., & Athar, T. (2009). Wet Synthesis of Copper Oxide Nanopowder. *International Journal of Green Nanotechnology: Materials Science & Engineering*, *1*(2), M67–M73. https://doi.org/10.1080/19430840903430220